LWT - Food Science and Technology 155 (2022) 112906

Contents lists available at ScienceDirect

LWT

journal homepage: www.elsevier.com/locate/lwt

Three-dimensional (3D) printability assessment of food-ink systems with superfine ground white common bean (*Phaseolus vulgaris* L.) protein based on different 3D food printers

Zhenxing Shi [a,b,c], Christophe Blecker [d], Aurore Richel [e], Zuchen Wei [a], Jingwang Chen [c,f], Guixing Ren [b], Dongqin Guo [a,*], Yang Yao [b,*], Eric Haubruge [c]

[a] Laboratory for Green Cultivation and Deep Processing of Three Gorges Reservoir Area's Medicinal Herbs, College of Biology and Food Engineering, Chongqing Three Gorges University, Chongqing 404120, People's Republic of China
[b] Institute of Crop Science, Chinese Academy of Agricultural Sciences (CAAS), 80 South Xueyuan Road, Haidian, Beijing, 100081, People's Republic of China
[c] Gastronomic Sciences Lab, University of Liege - Gembloux Agro-Bio Tech, 2 Passage des Déportés, Gembloux, 5030, Belgium
[d] Food Science and Formulation Lab, University of Liege - Gembloux Agro-Bio Tech, 2 Passage des Déportés, Gembloux, 5030, Belgium
[e] Biomass and Green Chemistry Lab, University of Liege - Gembloux Agro-Bio Tech, 2 Passage des Déportés, Gembloux, 5030, Belgium
[f] Lab of Food Chemistry and Nutrition Science, Institute of Food Science and Technology, Chinese Academy of Agricultural Sciences; Key Laboratory of Agro-products Processing, Ministry of Agriculture, No. 2 Yuan Ming Yuan West Road, Haidian District, Beijing, 100193, PR China

ARTICLE INFO

Keywords:
3D food printing
Superfine grinding
Common bean protein
Physical properties
α-AI activity

ABSTRACT

Three-dimensional (3D) printing technology is innovatively used in creating customized healthy food for different population groups. This study provided two appropriate food-ink systems with common bean protein extract (CBPE) for the syringe-based 3D food printer (0.5 g of sodium alginate, 6 g of gelatin, and 40 g of CBPE in 100 mL of water) and the gear-based 3D food printer (3.5 g of agar, 0.05 g of xanthan, and 12 g of CBPE in 100 mL of water), respectively. Superfine grinding significantly ($p < 0.05$) decreased the particle size of CBPE and resulted in a reduction in the printability mainly through increasing ($p < 0.05$) the adhesiveness and the swell powder of food-ink systems, respectively for the syringe-based 3D food printer and the gear-based 3D food printer. The decrease in the stability of printed products by the syringe-based 3D food printer was mainly due to the reduced water binding capacity ($p < 0.05$) by superfine grinding. Besides, the syringe-based 3D food printer was more suitable for printing CBPE based foods due to its weaker effects on the α-AI activity ($p < 0.05$). These findings were expected to provide new ideas for the potential application of white common bean protein in 3D food printing technology.

1. Introduction

Three-dimensional (3D) printing, also known as additive manufacturing, is an emerging technology to manufacture personalized products from digital models through layer-by-layer superposition and deposition of raw materials (Calignano et al., 2017). In the last decade, 3D printing technology has been adopted in the food engineering field and attracted accumulating interests, because of its potential advantages like the free design of shape, taste, texture, flavor and particularly nutritional composition (Chen et al., 2019; Yang, Zhang, Bhandari, & Liu, 2018). This technology makes it possible to create customized food to meet the unique requirements of various population groups. For instance, it can make suitable nutritional meals for children, seniors, and athletes who require highly nutritive foods such as high-quality protein, dietary fiber, and desirable fat (Hussain, Malakar, & Arora, 2021).

Extrusion-based printers are the most commonly used machines in commercial 3D food printing. During the extrusion process, four mechanisms are usually applied (Fig. 1). In the syringe-based extrusion system, the step motor impulses printable materials via a plunger inside the tube to pass through the nozzle tip. This system is initially designed for plastic material and is gradually modified to be suitable for printing most semi-solid food materials (Chen et al., 2019; F. Yang et al., 2018). In the gear-based extrusion system, food materials are pushed out by two reversely rotating gears at a controlled temperature. It is newly developed for those unique food materials which are originally liquid at a high temperature while become solid at a lower temperature in a short

* Corresponding authors.
E-mail addresses: guodongqin1997@163.com (D. Guo), yaoyang@caas.cn (Y. Yao).

https://doi.org/10.1016/j.lwt.2021.112906
Received 2 October 2021; Received in revised form 18 November 2021; Accepted 30 November 2021
Available online 1 December 2021

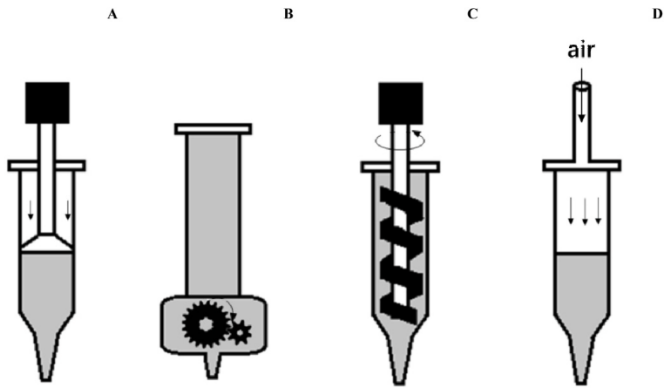

Fig. 1. The schematic diagrams of different types of extrusion-based 3D food printers. A-D represent the syringe-based extrusion system, the gear-based extrusion system, the screw-based extrusion system, and the air pressure-based extrusion system.

time. The screw-based extrusion is a system that mixes and pushes out food materials with a screw inside the tube, and is only suitable for semi-solid materials with low mechanical strength and viscosity (Liu, Zhang, Bhandari, & Yang, 2018). The air pressure-based extrusion system is similar to the syringe-based ones. It pushes materials by compressed air instead of the plunger. For all of these extrusion-based 3D printing systems, the ability of being printed out smoothly and self-supporting is the common requirement for the food materials, which heavily depends on their physical properties that include rheological property, gelling property, and textural property (Jiang et al., 2019). Therefore, the hotspot on 3D food printing is to modify food materials be applicable to various types of 3D food printers (Maniglia, Lima, Junior, Oge, & Le-Bail, 2020).

Previous studies demonstrated that α-amylase inhibitor (α-AI) isolated from white common bean (Phaseolus vulgaris L.), also called "starch blocker", is a glycoprotein with a molecular weight of about 36 kDa, which can inhibit adipocyte differentiation in vitro, and modulate the gut microbiotas composition of obese rats (Chokshi, 2006; Shi, Zhang, Zhu, Yao, & Ren, 2021; Shi et al., 2020; M. Y. Yang et al., 2008). Nowadays, white common bean protein has become a potential raw material to produce customized healthy food for obese or diabetic people, due to the α-AI enriched in it. However, at present, the assessment of the 3D printability of white common bean protein is limited. In general, plant proteins are preferable printable materials due to their proper rheological property and gelling property (Holland, Tuck, & Foster, 2018). In the pre-experiments, we found that simple white common bean protein gel was able to be printed out both by the syringe-based extrusion printer and the gear-based extrusion printer. But the printed products were unsound and prone to collapse. Several studies have uncovered that self-supporting ability of protein-based food-ink system was improved by enhancing the gel networks (Hussain et al., 2021). Gelation temperature and shear-thinning behavior were enhanced by addition the hydrocolloids (Liu, Bhesh, Sangeeta, Sylvester, & Min, 2018). Gel strength and gel hardness were promoted through increasing the calcium concentration (Zhang, Lou, & Schutyser, 2018). In addition, the association of particle size distribution with the physical properties of protein-based gel has also been well established. The rheological property, gelling property, solubility and protein surface hydrophobicity were significantly improved by decreased particle size of whey protein using superfine grinding (Sun et al., 2015, 2016). However, the modification for 3D printing application of white common bean protein-based gel is still under-explored in the literature, considering addition of hydrocolloids and using superfine grinding method. Besides, α-AI easily loses its activity due to the thermal instability (Zi et al., 2015), it is still unknown that how 3D printing process will affect the α-AI activity of white common bean protein.

Based on this context, the purposes of this research were (1) to assess the 3D printability of the food-ink systems with superfine ground white common bean protein extract (CBPE) and hydrocolloids based on two extrusion-based printers, (2) to explain the changes in the 3D printability of food-ink systems caused by superfine grinding through evaluating the rheological, hydration and textural properties; and (3) to clarify the influence of 3D printing process on the α-AI activity of CBPE.

2. Materials and methods

2.1. Materials

CBPE powder was purchased from Xi'an Weite Biological Technology Co. (Shanxi, China), and ground to <0.15 mm (100-mesh sieve). Porcine pancreatic α-amylase was purchased from Sigma Chemical Co. (St. Louis, MO, USA). Gelatin and alginate sodium were purchased from Atlas Ltd. (Harelbeke, West Flanders, Belgium). Agar and xanthan were purchased from MCC Trading International (Dusseldorf, Germany). Other chemical reagents used were of analytical grade.

2.2. Superfine grinding and characterization of CBPE

The superfine grinding of CBPE was performed using a superfine grinder (WFM20, Jiangyin Youxie Machinery Manufacturing Co., Ltd., Jiangyin, China) for 0 min (N), 6 min (S-6), 12 min (S-12), and 24 min (S-24), respectively.

The characterization of superfine ground CBPE was performed by determining the nutritional composition, particle size distribution, and α-AI activity. The contents of protein, fat, total carbohydrates, ash and moisture were determined according to the Kjeldahl method (NY/T 3–1982), AOAC 1990, phenol-sulfuric acid method, combustion method, and constant weight method, respectively (Zhu et al., 2020). The particle size distribution of different samples was determined using a dry powder particle size NKT2010-L detector (Shandong NKT Analytical Instruments Co., Ltd., China) equipped with a laser beam. The D_{10}, D_{50}, and D_{90} value were recorded, and the particle size width span was estimated with the equation: $Span=(D_{90}-D_{10})/D_{50}$. The α-AI activity of different samples was evaluated as previously reported (Yao, Hu, Zhu, Gao, & Ren, 2016).

2.3. Preparation of food-ink systems for two types of 3D printers

The suitable food-ink system adopted for the syringe-based 3D printer (Formula A) were obtained according to our previous report with some modifications based on the pre-experiments (Chen et al., 2019) (**Supplementary materials**, Table S1). Briefly, the alginate sodium solution was prepared by dissolving alginate sodium in distilled water stirring for 2 h to a final concentration of 0.5% (w/v). Gelatin was added to the alginate sodium solution to reach a concentration of 6.0% (w/v). The mixture was incubated in a 45 °C water bath for 1 h. Then, CBPE (N) was added to the alginate and gelatin mixed solution to reach a final concentration of 40% (w/v), and stirred at approximately 100 rpm for 5 min. After storage at 4 °C overnight, the suitable food-ink system (NAG) was obtained. To assess the effect of superfine grinding, CBPE was replaced by S-6, S-12 and S-24, respectively, to prepare undertest food-ink systems named S-6AG, S-12AG, and S-24AG.

The suitable food-ink system adopted for the gear-based 3D printer (Formula B) was prepared based on the pre-experiments (**Supplementary materials**, Table S1). Briefly, the agar and xanthan were added to distilled water at concentrations of 3.5% (w/v) and 0.05% (w/v), respectively, at room temperature with stirring for 40 min. Then CBPE (N) was added to the agar and xanthan mixed solution to reach a concentration of 12% (w/v) with stirring for 5 min to obtain the food-ink system (NAgX). To assess the effect of superfine grinding, CBPE was replaced by S-6, S-12 and S-24, respectively, to prepare undertest food-ink systems named NAgX, S-6AgX, S-12AgX, and S-24AgX.

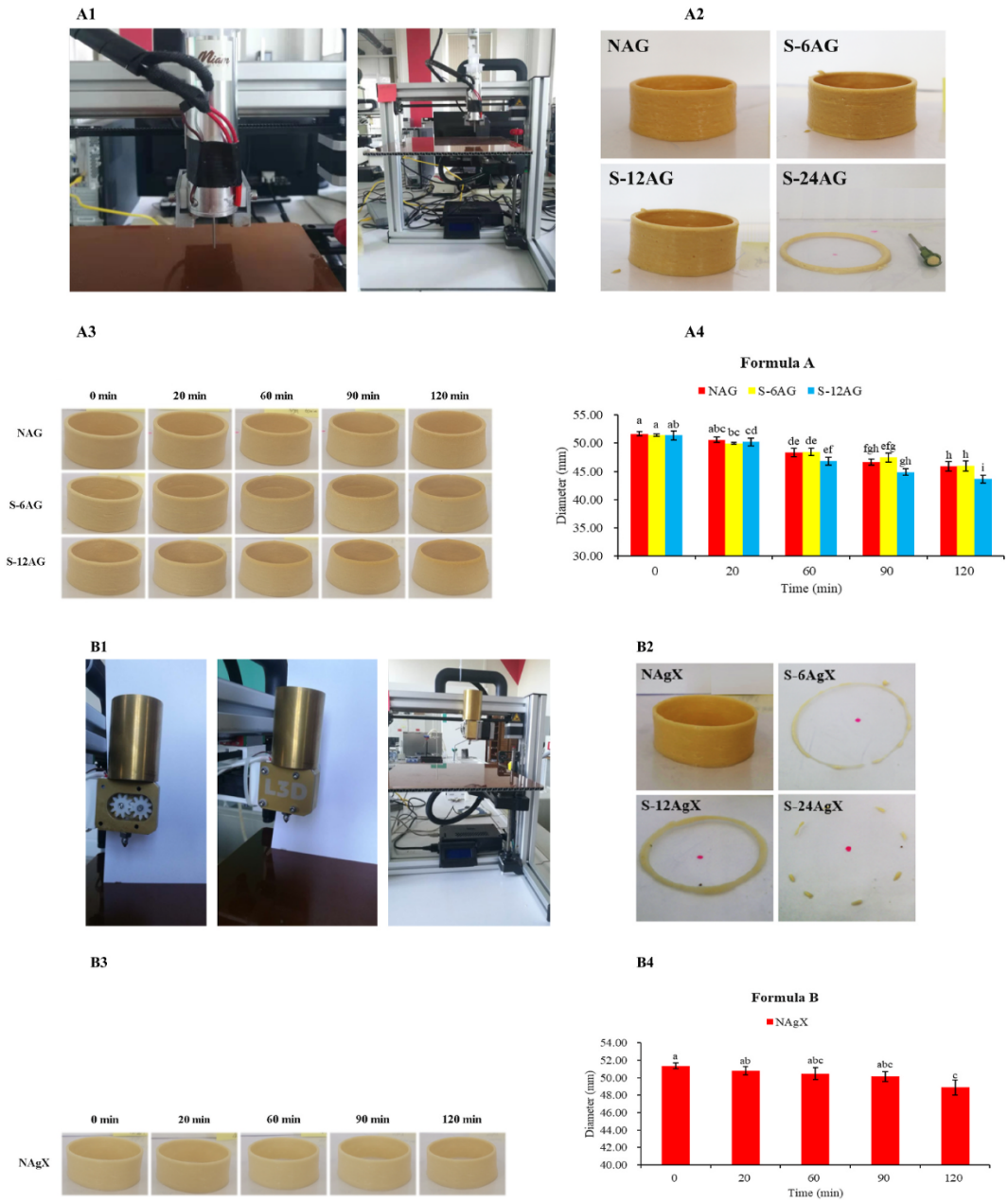

Fig. 2. Three-dimensional print performance of food-ink systems. A1-A4 and B1–B4 represent the photographs 3D printer (A1 and B1), the printed products (A2 and B2), the stability of printed products (A3 and B3), and the deformation details of printed products (A4 and B4) for Formula A and Formula B, respectivey. Different letters superscripted on the results were significantly different at $p < 0.05$. Abbreviation: CBPE, common bean protein extract; N, normal common bean protein powder; S-6, superfine grinding for 6 min, S-12, superfine grinding for 12 min; S-24, superfine grinding for 24 min; NAG, the mixture of N, alginate and gelatin; S-6AG, the mixture of S-6, alginate and gelatin; S-12AG, the mixture of S-12, alginate and gelatin; S-24AG, the mixture of S-24, alginate and gelatin; NAgX, the mixture of N, agar and xanthan; S-6AgX, the mixture of S-6, agar and xanthan; S-12AgX, the mixture of S-12, agar and xanthan; S-24AgX, the mixture of S-24, agar and xanthan.

2.4. Printing process in two types of 3D food printers

The 3D printing of Formula A was performed using a syringe-based 3D printer (3.0 Felix, Netherlands) as shown in Fig. 2. A1. The prepared food-ink systems were heated to 35 °C by a water bath and were carefully loaded into the syringe. Then the materials were printed out continuously from the nozzle tip by a plunger, and the designed shape was deposited layer-by-layer. The maximum volume of the syringe was approximately 60 mL, and a nozzle tip with a diameter of 1.55 mm was used. A hollow cylinder (length × width × height = 50 × 50 × 20 mm) was designed by the open-source software CURA 15.04.6 (Ultimaker B. V., Netherlands). The key parameters of the 3D printer include layer height (mm), shell thickness (mm), printing speed (mm/s), flow rate (%), and printing temperature (°C) were fixed at 0.6 mm, 1.55 mm, 10 mm/s, 80%, and 35 °C, respectively.

The 3D printing of Formula B was performed using a gear-based 3D printer (L3D Extruder Kit, Choco, Ukraine) as shown in Fig. 2. B1. A total of 30–40 mL of prepared food-ink systems were heated to 90 °C and immediately put into the L3D Extruder Kit before cooled to 70 °C. The materials were printed out from the nozzle tip by two gears which are reversely rotated, according to the designed shape. The maximum volume of the kit is approximately 50 mL, and the diameter of the nozzle tip is 0.5 mm. A hollow cylinder (length × width × height = 50 × 50 × 20 mm) was designed by the open-source software CURA 15.04.6

Table 1
The nutritional composition, particle size distribution and α-AI activity of superfine grinded CBPE[a,b].

Sample	Nutritional composition					Particle size distribution				α-AI activity (U g^{-1})
	Protein (%)	Total Carbohydrates (%)	Fat (%)	Ash (%)	Moisture (%)	D_{10} (μm)	D_{50} (μm)	D_{90} (μm)	Span	
N	76.25 ± 0.07[a]	4.75 ± 0.02[a]	5.60 ± 0.28[a]	0.49 ± 0.01[a]	11.34 ± 0.59[a]	2.6 ± 0.14[a]	37.43 ± 2.08[a]	74.1 ± 1.06[a]	1.91 ± 0.08[bc]	961.30 ± 29.43[a]
S-6	76.91 ± 0.09[a]	4.68 ± 0.04[a]	5.59 ± 0.19[a]	0.48 ± 0.04[a]	11.89 ± 0.78[a]	1.3 ± 0.01[b]	3.42 ± 0.09[b]	21.43 ± 1.73[b]	5.9 ± 0.66[a]	938.93 ± 33.86[a]
S-12	76.49 ± 0.08[a]	4.88 ± 0.09[a]	5.62 ± 0.09[a]	0.51 ± 0.02[a]	11.56 ± 0.51[a]	1.06 ± 0.03[c]	2.27 ± 0.05[b]	7.3 ± 1.58[c]	2.76 ± 0.75[b]	958.61 ± 30.84[a]
S-24	76.37 ± 0.06[a]	4.77 ± 0.05[a]	5.57 ± 0.22[a]	0.47 ± 0.03[a]	11.66 ± 0.49[a]	0.97 ± 0.03[c]	2.05 ± 0.06[b]	3.73 ± 0.03[d]	1.35 ± 0.04[c]	964.92 ± 28.64[a]

[a] Data are expressed as mean ± standard deviation of triplicate samples.
[b] Different letters superscripted on the results were significantly different at $p < 0.05$.

(Ultimaker B.V., Netherlands). The printing parameters were fixed at a layer height of 0.6 mm, a shell thickness of 0.8 mm, a printing speed of 10 mm/s, a flow rate of 50%, and a printing temperature of 70 °C.

After printing, the samples were covered with an aluminum specimen box and stored under refrigeration (4 °C) to avoid dehydration. The diameters of the printed products were measured, after printing for 0, 20, 60, 90 and 120 min at room temperature by a vernier caliper.

2.5. Rheological property

The rheological property of food-ink systems was determined using a rheometer (DHR-1, TA Instruments, USA) according to our previous method with some modifications (Chen et al., 2019). The steady flow property of different food-ink systems was examined in terms of the viscosity as a function of shear rate from 0.01 to 100 s^{-1}. For samples in Formula A, the operating temperature was 35 °C. For samples in Formula B, the operating temperature was 70 °C. The temperature sweep of food-ink systems was conducted at a frequency of 1 Hz. For samples in Formula A, the viscosity, storage modulus (G′), loss modulus (G′′), and loss tangent (tan δ) in the temperature range of 4–50 °C with a heating rate of 1 °C/min at a constant shear strain of 0.5% were obtained. For samples in Formula B, the temperature range was set from 5 °C to 100 °C. The frequency sweep property of food-ink systems was evaluated by changing the frequency from 0.1 to 100 Hz at a constant strain of 0.5%. The G′, G′′ and tan δ were recorded. For samples in Formula A and Formula B, the operating temperature was 35 °C and 70 °C, respectively. All measurements were repeated three times.

2.6. Textural property

The textural property of food-ink systems was measured using a TMS-PRO texture analyzer (FTC, Virginia, USA). Samples were prepared as described in section 2.3 and were arranged adjacent to each other on the operating platform. The test conditions were as follows: texture profile analysis (TPA) mode; probe selection, P/50; parameter settings of pretest speed, test speed, and posttest speed of TPA were 1.00, 1.00, and 1.00 mm/s, respectively; test compression rate of TPA, 75%; test distance, 20.0 mm; trigger force, 5 g. All measurements were repeated three times.

2.7. Hydration property

The swelling power (SP) was determined as follows (Nagar, Sharanagat, Kumar, Singh, & Mani, 2019): Three grams of prepared food-ink systems were mixed in 50 mL distilled water (W0). Samples in Formula A and samples in Formula B were respectively incubated in a water bath at 35 °C and 70 °C for 30 min under constant stirring, and then immediately cooled to room temperature under tap water. The supernatants were obtained by centrifugation at 8000×*g* for 20 min and the precipitates were weighed (W1), and SP was calculated using the following equation:

$$SP = W1/W0 \quad (1)$$

The water binding capacity (WBC) was determined as follows (Ulfa, Putri, Fibrianto, Prihatiningtyas, & Widjanarko, 2020): Three grams (W2) of prepared food-ink systems were centrifuge at 5000×*g* for 20 min at 4 °C. The excess water was removed, and the precipitates was weighted (W3) and calculated using following equation:

$$WBC = W3/W2 \quad (2)$$

2.8. α-AI activity

The α-AI activity of printed products was evaluated according to our previous report with some modifications (Yao et al., 2016). Briefly, the printed products were freeze-dried and milled passed through a 60-mesh sieve. The α-amylase solution (6.5 U mL^{-1}) was prepared by dissolving porcine pancreatic α-amylase in PBS buffer (pH 7.45). Two hundred microliter of α-amylase solution was mixed with 200 μL of CBPE equivalent (1 mg/mL) samples, and the mixture was incubated in a water bath at 37 °C for 10 min. Then, 200 μL of 2% (w/v) soluble starch solution was added to the mixture and the reaction was kept going for 10 min. Then, 1 mL of 3,5-dinitrosalicylic acid was added to the mixture. And the mixture was kept in a boiling water bath for 5 min. The volume of the mixture was finally increased to 6 mL with double-distilled water. A sample blank measurement was performed simultaneously with the inhibitor but without enzyme. One inhibitory unit was defined as the amount of α-AI that completely inhibited the activity of one unit of enzyme.

2.9. Statistics

Values were expressed as the means ± standard deviation (SD). One-way ANOVA, followed by the Tukey post-hoc test, was used to analyze the results by SPSS (Statistical Package for Social Science) version 17.0. The significance of differences was set to $p < 0.05$.

3. Results and discussion

3.1. Characterization of CBPE

The effects of superfine grinding on the nutritional composition, particle size distribution and α-AI activity of CBPE were presented in Table 1. Protein purity of the commercially available CBPE was 76.25%, and the rest of the components consisted of carbohydrates, fat, ash and moisture. No significant difference ($p > 0.05$) in the contents of protein, total carbohydrates, fat, ash and moisture was observed among four samples, which suggested that the superfine grinding process did not

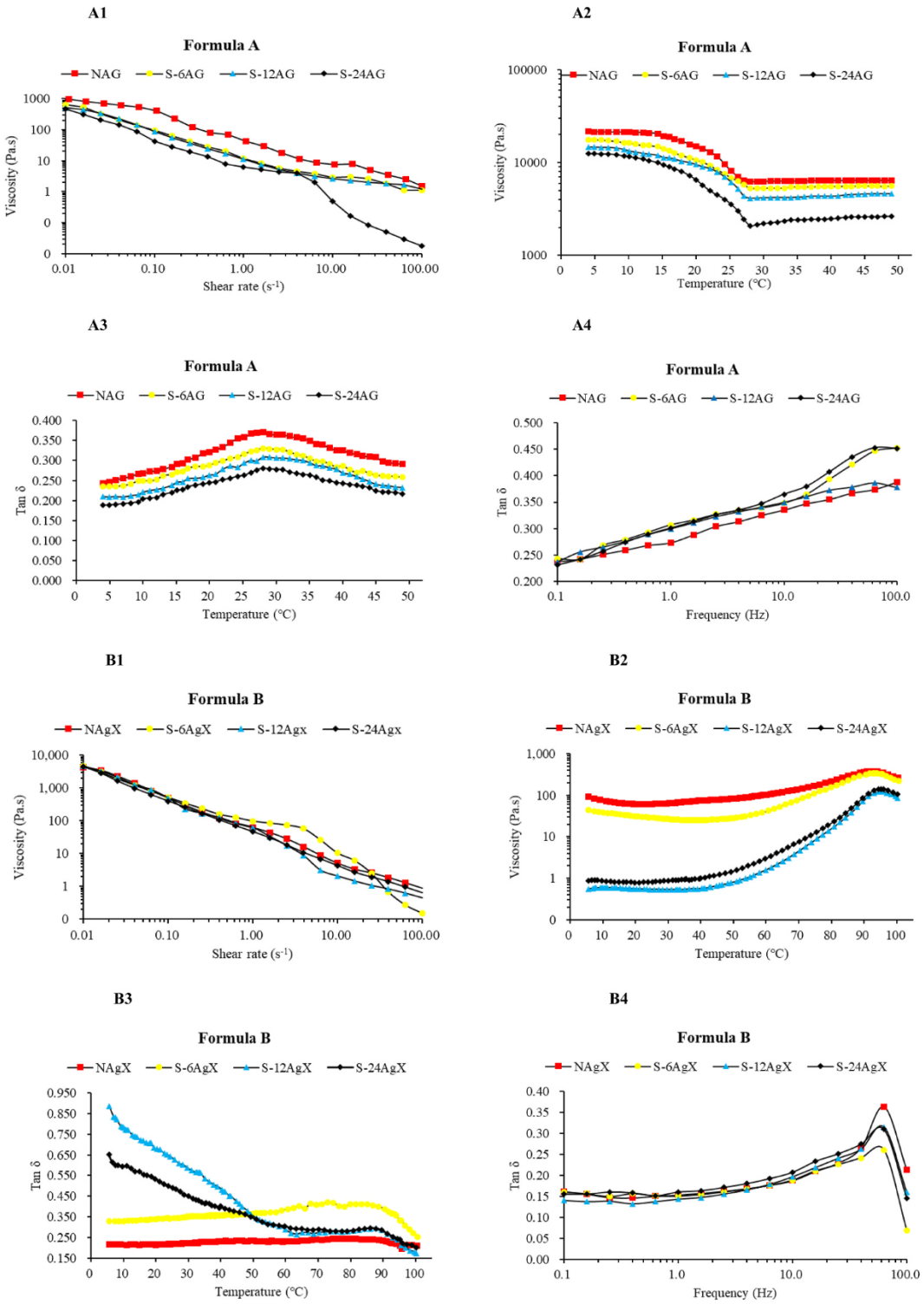

Fig. 3. Rheological properties of CBPE mixtures. A1-A4 and B1–B4 represent the changes in viscosity with shear rate sweep (A1 and B1), the changes in viscosity with temperature sweep (A2 and B2), the tangent (tan δ = G″/G′) with temperature sweep (A3 and B3), and the tangent (tan δ = G″/G′) with frequency sweep (A4 and B4) for Formula A and Formula B, respectivey. Abbreviation: CBPE, common bean protein extract; N, normal common bean protein powder; S-6, superfine grinding for 6 min, S-12, superfine grinding for 12 min; S-24, superfine grinding for 24 min; NAG, the mixture of N, alginate and gelatin; S-6AG, the mixture of S-6, alginate and gelatin; S-12AG, the mixture of S-12, alginate and gelatin; S-24AG, the mixture of S-24, alginate and gelatin; NAgX, the mixture of N, agar and xanthan; S-6AgX, the mixture of S-6, agar and xanthan; S-12AgX, the mixture of S-12, agar and xanthan; S-24AgX, the mixture of S-24, agar and xanthan.

change the nutritional composition of CBPE. It was reported that, as an important factor, particle size influenced the physical properties of protein (Guo, Guan, Ke, & Zhan, 2015). The present results showed that, after superfine grinding, the particle size of CBPE was reduced evidenced by the changes in D_{10}, D_{50}, and D_{90} values, which were consistent with the previous study of Sun et al. (Sun et al., 2016). The D_{50} values of CBPE decreased from 37.43 to 3.42, 2.27, and 2.05 μm, after superfine grinding for 6, 12, and 24 min, respectively, which

indicated that the superfine ground CBPE belong to superfine food powder grade (Hu, Chen, & Ni, 2012). A larger Span value indicates a wider particle size distribution (Huang, Liang, Liu, Qiu, & Zhu, 2020). The present results of Span values further explored the effects of superfine grinding duration on the particle size distribution of CBPE. As shown, though 6 min of superfine grinding decreased the particle size, it significantly widened ($p < 0.05$) the particle size distribution. With the extension of the superfine grinding duration, the particle size distribution became uniform. There was no significant difference ($p > 0.05$) among the four samples in α-AI activity, which suggested that superfine grinding have no obvious effect on the α-AI activity of CBPE.

3.2. Effects of superfine grinding of CBPE on the printability of food-ink systems based on two types of 3D food printers

A suitable food-ink system with CBPE and hydrocolloids (0.5 g of sodium alginate, 6 g of gelatin, and 40 g of CBPE in 100 mL of water) was established for the syringe-based 3D printer. To evaluate how superfine grinding affect the printability, CBPE was replaced by S-6, S-12, and S-24, respectively. As shown in Fig. 2. A2, food-ink systems including NAG, S-6AG and S-12AG were able to be printed out continuously from the nozzle tip and the designed hollow cylinder was successfully deposited layer-by-layer. However, S-24AG blocked the nozzle and could not be printed out by the syringe-based 3D printer. As previously reported, the final products were defined as successful printings if they maintained their shapes for 20 min after printing (Fan, Zhang, Liu, & Ye, 2020). The stability of printed products was further assessed, we can see from Fig. 2. A3 that deformation occurred in all the printed products, during 120 min of storage. The quantitative results (Fig. 2. A4) showed that, for the printed product with NAG, there is no significant difference ($p > 0.05$) in the diameters at 0 min and 20 min. However, the diameters of the printed products with S-6AG and S-12AG significantly decreased ($p < 0.05$), after 20 min of storage. This might be because the gelatin-alginate and peptide chain mixture linked together to form a network gel structure and bind moisture to itself (Chen et al., 2019), and the gel structure maintained its shape and supported its own weight in the short time. After 120 min, the diameters of printed products with NAG, S-6AG and S-12AG were reduced by 11.22%, 10.51%, and 15.01%, respectively.

It was reported that agar and xanthan showed synergistic effects on gel formation, which would contribute to maintaining the shape of 3D printed products (Gao, Dai, Chen, Xie, & Yue, 2017). In addition, the viscosity of agar-based gel depends heavily on environment temperature. Therefore, agar and xanthan were selected to improve the printability of CBPE in gear-based extrusion system. After a suitable food-ink system with CBPE (3.5 g of agar, 0.05 g of xanthan, and 12 g of CBPE in 100 mL of water) was established, S-6, S-12, and S-24 were used to replace CBPE, respectively. However, as shown in Fig. 2. B2 and Fig. 2. B3, only NAgX was able to be printed out and the printed product showed excellent stability. As shown in Fig. 2. B4, the diameter had no significant decrease, after 90 min of storage. This might be caused by the property of agar to form strong gels in aqueous solutions, and after cooling from high temperature, the agar solutions were initiated by a coil-to-helix transition, followed by the aggregation of the helices to form a network structure (Dai & Matsukawa, 2012).

These results above indicated that superfine grinding of CBPE did affect the printability of food-ink systems both in the syringe-based 3D printer and the gear-based 3D printer. This phenomenon remained to be explained through determination of the physical properties.

3.3. Effects of superfine grinding of CBPE on the rheological property of food-ink systems

To a certain extent, rheological property determines the printability of food materials in the 3D printing process (Zhu, Stieger, van der Goot, & Schutyser, 2019). In general, viscous food materials should have appropriate viscosity to go through the nozzle of a 3D printer and stick together layer by layer (Liu, et al., 2018).

3.3.1. Shear rate sweep

Both Fig. 3. A1 and Fig. 3. B1 showed that all of the food-ink systems had shear-thinning behavior. This result indicated that the mixtures of CBPE and hydrocolloids were pseudoplastic liquids, where the viscosity was low at a high shear rate to make extrusion of materials from the nozzle easier (C. P. Lee, Karyappa, & Hashimoto, 2020). As shown in Fig. 3. A1, the viscosities of S-6AG, S-12AG and S-24AG were lower than that of NAG, which suggested that superfine grinding enhanced the shear-thinning behavior. Similar results were discovered in whey protein, soy protein and egg white protein isolates, it has reported that, with the reduction in particle size of the protein, the viscosity decreased accordingly, which might be caused by the entanglement and intermolecular interactions among polymer molecules (Arzeni et al., 2012; Wang et al., 2020). As shown in Fig. 3. B1, the viscosities of S-6AgX, S-12AgX and S-24AgX were similar to that of NAgX, which could be attributed to the different protein contents between the two formulas.

3.3.2. Temperature sweep

As shown in Fig. 3. A2, with the increasing temperature, the viscosities of NAG, S-6AG, S-12AG and S-24AG reduced, and when the temperature exceeded approximately 28 °C, the viscosities maintained at a low level, which was consistent with our previous study (Chen et al., 2019). As shown in Fig. 3. B2, the increased temperature led to a rapid increase in the viscosity curves from 5 °C to 95 °C, and viscosities then decreased from 95 °C to 100 °C. The peaks presented at approximately 95 °C, which might be caused by the addition of agar (Dai & Matsukawa, 2012). Agar particles began to gradually dissolve in water, and the viscosity of the solution increased with the temperature rosing from 5 °C to 95 °C. When the temperature was higher than 95 °C, the dissolved agar particles began to present the liquid state, and the viscosity of the solution decreased. From the two figures, S-6AG, S-12AG, and S-24AG showed lower viscosity than NAG, and S-6AgX, S-12AgX, and S-24AgX showed lower viscosity than NAgX. These results suggested that superfine grinding did affect the viscosities of food-ink systems at different temperatures.

3.3.3. The storage modulus (G′) and loss modulus (G″)

The G′ and G″ represent the elasticity and viscous properties of the materials, respectively (Lee, Won, Kim, & Park, 2019). Fig. S1. A1-A2 and Fig. S1. B1–B2 showed the curves of G″ or G′ based on temperature sweeps. Fig. S1. A3-A4 and Fig. S1. B3–B4 showed the curves of G″ or G′ based on frequency sweeps. The loss tangent ($\tan\delta = G''/G'$) can be used to analyze the elastic behavior ($\tan\delta < 1$) or viscous behavior ($\tan\delta > 1$) (Chen et al., 2019; F. Yang et al., 2018). Fig. 3. A3 and B3 showed the tan δ at different temperatures. The tan δ value of all food-ink systems were lower than 1, which indicated that they all had fluidity. For NAG, S-6AG, S-12AG, and S-24AG, there were positive peaks at approximately 28 °C, which might be due to the gelatin and peptides uniting and forming a highly ramified three-dimensional network, and the fluid semi-gel was converted into an elastic gel or "solid" at a lower temperature (Chen et al., 2019). NAgX, S-6AgX, S-12AgX, and S-24AgX (Fig. 3. B3) showed liquid-like state from 50 °C to 100 °C. Consistent with the tan δ values at different temperatures, all the tan δ values at different frequencies were also lower than 1 (Fig. 3. A4 and B4). For NAgX, S-6AgX, S-12AgX, and S-24AgX, the curves of tan δ had peaks presented at 63.1 Hz (396.44 rad/s). It was possible that the softer agar samples could no longer be approximated as linearly viscoelastic when the frequency was below 100 Hz or above 200 Hz (Nayar, Weiland, Nelson, & Hodge, 2012). Chen, Zhang, and Phuhongsung (2021) reported that five protein, no matter vegetable and animal proteins, the values of G'' are higher than G′; especially the tan δ values of vegetable proteins (such as peanut, pea and wheat hydrolyzed proteins) were all lower than 1, showing elastic behavior in dynamic mechanical

Table 2
The texture analysis result of different CBPE mixtures [a,b].

Sample		Hardness (g)	Adhesiveness (g·sec)	Springiness	Cohesiveness	Gumminess	Resilience
Formula A	**NAG**	269.33 ± 4.78^{A}	-78.87 ± 1.4^{A}	0.81 ± 0.02^{B}	0.63 ± 0.02^{AB}	160.33 ± 6.31^{A}	0.12 ± 0^{AB}
	S-6AG	240.13 ± 16.9^{A}	-85.03 ± 4.84^{A}	0.9 ± 0.06^{A}	0.67 ± 0.04^{A}	161.89 ± 31.72^{A}	0.12 ± 0^{B}
	S-12AG	263.35 ± 17.26^{A}	-80.14 ± 6.56^{A}	0.71 ± 0.02^{C}	0.58 ± 0.04^{B}	151.56 ± 21.55^{A}	0.13 ± 0.01^{AB}
	S-24AG	189.16 ± 8.27^{B}	-146.78 ± 4.97^{C}	0.89 ± 0.01^{AB}	0.7 ± 0.02^{A}	128.56 ± 5.3^{A}	0.14 ± 0.01^{A}
Formula B	**NAgX**	287.23 ± 15.63^{a}	-23.37 ± 0.87^{a}	0.49 ± 0.01^{a}	0.28 ± 0^{ab}	78.19 ± 3.09^{a}	0.06 ± 0^{a}
	S-6AgX	267.02 ± 9.68^{a}	-21.37 ± 0.58^{a}	0.52 ± 0.07^{a}	0.31 ± 0.04^{a}	71.36 ± 10.53^{a}	0.05 ± 0^{a}
	S-12AgX	290.59 ± 15.42^{a}	-21.76 ± 1.03^{a}	0.44 ± 0.07^{a}	0.24 ± 0^{b}	72.25 ± 4.02^{a}	0.05 ± 0^{a}
	S-24AgX	199.81 ± 13.88^{b}	-30.05 ± 2.12^{b}	0.48 ± 0.05^{a}	0.3 ± 0.04^{ab}	58.19 ± 12.73^{a}	0.06 ± 0^{a}

[a] Data are expressed as mean ± standard deviation of triplicate samples.
[b] Means in a column with different letters differ significantly ($p < 0.05$).

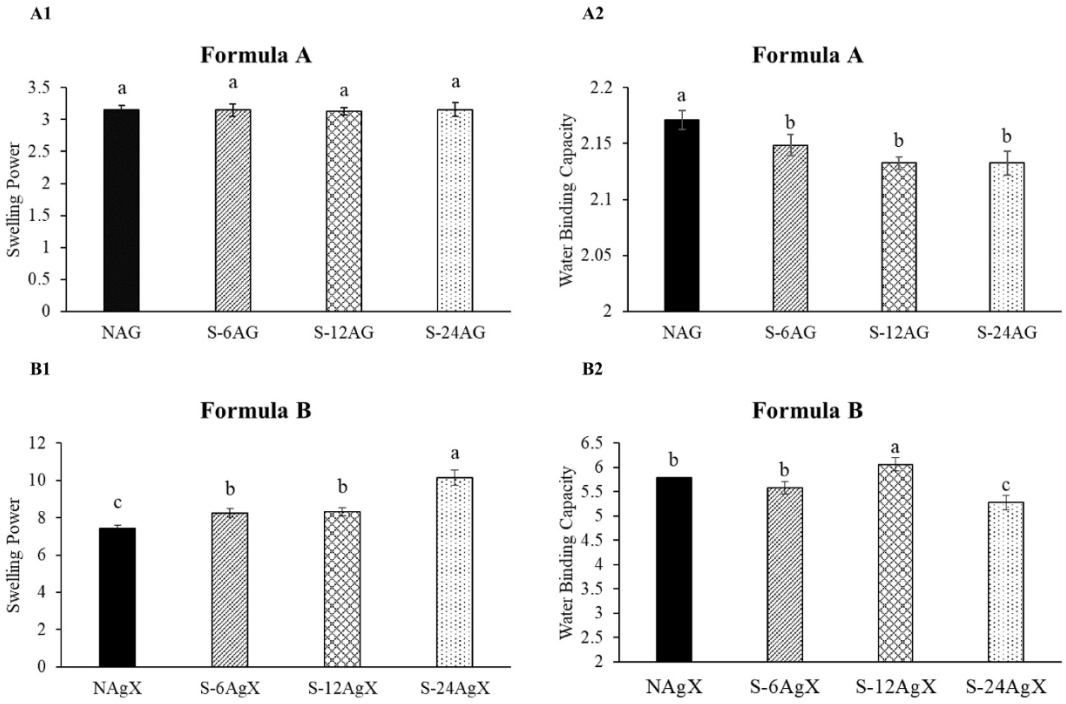

Fig. 4. The hydration property of CBPE mixtures. A1-A2 and B1–B2 represent the swelling power (A1 and B1) and water binding capacity (A2 and B2) for Formula A and Formula B, respectivey. Different letters superscripted on the results were significantly different at $p < 0.05$. Abbreviation: CBPE, common bean protein extract; N, normal common bean protein powder; S-6, superfine grinding for 6 min, S-12, superfine grinding for 12 min; S-24, superfine grinding for 24 min; NAG, the mixture of N, alginate and gelatin; S-6AG, the mixture of S-6, alginate and gelatin; S-12AG, the mixture of S-12, alginate and gelatin; S-24AG, the mixture of S-24, alginate and gelatin; NAgX, the mixture of N, agar and xanthan; S-6AgX, the mixture of S-6, agar and xanthan; S-12AgX, the mixture of S-12, agar and xanthan; S-24AgX, the mixture of S-24, agar and xanthan.

analyze. Our results were consistent (tan δ < 1), but the tan δ are different from various vegetable proteins, which may due to different protein particles water binding ability or degree (Tarhan, Spotti, Schaffter, Corvalan, & Campanella, 2016). It indicated that as printing ink, different type of proteins may show various printing properties.

3.4. Effects of superfine grinding of CBPE on the textural property of food-ink systems

As shown in Table 2, the hardness, adhesiveness, springiness, cohesiveness, gumminess and resilience of food-ink systems were determined. Adhesiveness is also regarded as stickiness and has a significant impact on the binding strength of printed layers (Nida, Anukiruthika, Moses, & Anandharamakrishnan, 2021). Though stronger adhesiveness of materials could help to mold 3D printed products, it makes materials easier to block nozzles. The present results showed that the adhesiveness of S-24AG (−146.78 g s) was significantly stronger ($p < 0.05$) than that of NAG (−78.78 g s), S-6AG (−85.03 g s) and S-12AG (−80.14 g s), which might explain the failed 3D printing of S-24AG.

3.5. Effects of superfine grinding of CBPE on the SP and WBC of food-ink systems

The SP and WBC of food-ink systems were shown in Fig. 4. There was no significant difference ($p > 0.05$) in SP among NAG, S-6AG, S-12AG, and S-24AG (Fig. 4. A1), while the WBC of S-6AG, S-12AG, and S-24AG were significantly lower ($p < 0.05$) than NAG (Fig. 4. A2). Liu et al. (2021) reported that higher WBC of materials helped to lock more moisture in the food and reduced food shrinkage caused by dehydration (Liu et al., 2021). This could be explained that the printed products from S-6AG and S-12AG were easier to lose moisture than NAG and occurred more obvious deformation. As shown in Fig. 4. B1, S-6AgX, S-12AgX and S-24AgX presented much higher SP than NAgX ($p < 0.05$), which led to an expansion of the food-ink systems when passing through the nozzle tip, thus resulting in failed 3D printing process. These results agreed with Ullah et al. (2018) who claimed that material with smaller particle size had higher SP (Ullah et al., 2018). As shown in Fig. 4. B2, the WBC of NAgX was strong, which might explain the stability of the printed products from NAgX.

Table 3
α-AI activity in different 3D printed products based CBPE [a,b].

Samples		Total activity (U g^{-1})
Formula A	NAG	968.56 ± 24.30[a]
	S-6AG	964.02 ± 24.49[a]
	S-12AG	965.88 ± 11.19[a]
Formula B	NAgX	ND

[a] Data are expressed as mean ± standard deviation of triplicate samples.
[b] Means in a column with different letters differ significantly ($p < 0.05$).

3.6. Effects of 3D printing on the α-AI activity of CBPE

The α-AI activity of 3D printed products was measured. As shown in Table 3, printed products by the syringe-based 3D printer from NAG, S-6AG, and S-12AG showed similar α-AI activity ($p > 0.05$), which suggested that the syringe-based process had no influence on the α-AI activity of CBPE. However, the α-AI activity of printed products by the gear-based 3D printer from NAgX was undetected, which might be caused by the high environment temperature the presented during printing process. Zi et al. (2015) reported that the α-AI protein rapidly loses activity when the temperature was above 80 °C (Zi et al., 2015).

4. Conclusions

In this study, a suitable food-ink system with sodium alginate (0.5 g), gelatin (6 g), and CBPE (40 g) was established for the syringe-based 3D food printer, and a suitable food-ink system with agar (3.5 g), xanthan (0.05 g), and CBPE (12 g) was established for the gear-based 3D food printer. Superfine grinding of CBPE resulted in a reduction in the printability of food-ink systems and a reduction in the stability of printed products for the syringe-based 3D food printer, mainly through increasing their adhesiveness and lowering their WBC. Superfine grinding of CBPE also resulted in a reduction in the printability of food-ink systems for the gear-based 3D food printer, mainly through increasing their SP. CBPE in printed products by the syringe-based 3D food printer kept the α-AI activity, however, it lost the α-AI activity after the gear-based extrusion process. These findings were expected to provide new ideas for the potential application of white common bean protein in 3D food printing technology.

CRediT authorship contribution statement

Zhenxing Shi: Conceptualization, Methodology, Writing – original draft, Software. **Christophe Blecker:** Methodology, Writing – review & editing. **Aurore Richel:** Supervision, Writing – review & editing. **Zuchen Wei:** Methodology, Investigation. **Jingwang Chen:** Investigation. **Guixing Ren:** Supervision. **Yang Yao:** Writing – review & editing, Methodology, Data curation. **Eric Haubruge:** Writing – review & editing, Methodology, Supervision.

Declaration of competing interest

We declare that we do not have any commercial or associative interest that represents a conflict of interest in connection with the work submitted.

Acknowledgements

This work was supported by the earmarked fund for China Agricultural Research System of MOF and MARA (CARS-08-G20) (Food Legumes), Central Public-interest Scientific Institution Basal Research Fund (Y2020PT30) and China Scholarship Council (CSC). I also thank my friends, Sami Yunus and Simon De Jaeger give me many helps on my 3D printing experiment during my lab time in Gembloux, we have great friendships and wonderful memories in Belgium.

Abbreviations

CBPE	common bean protein extract
A	alginate
Ag	agar
G	gelatin
G′	storage modulus
G″	loss modulus
CBPE	common bean protein extract
N	normal grinding CBPE powder
S-6	superfine grinding for 6 min
S-12	superfine grinding for 12 min
S-24	superfine grinding for 24 min
NAG	the mixture of N, alginate and gelatin
S-6AG	the mixture of S-6, alginate and gelatin
S-12AG	the mixture of S-12, alginate and gelatin
S-24AG	the mixture of S-24, alginate and gelatin
NAgX	the mixture of N, agar and xanthan
S-6AgX	the mixture of S-6, agar and xanthan
S-12AgX	the mixture of S-12, agar and xanthan
S-24AgX	the mixture of S-24, agar and xanthan
SP	swelling power
WBC	water binding capacity

Appendix A. Supplementary data

Supplementary data to this article can be found online at https://doi.org/10.1016/j.lwt.2021.112906.

References

Arzeni, C., Martínez, K., Zema, P., Arias, A., Pérez, O. E., & Pilosof, A. M. R. (2012). Comparative study of high intensity ultrasound effects on food proteins functionality. *Journal of Food Engineering, 108*, 463–472.
Calignano, F., Manfredi, D., Ambrosio, E. P., Biamino, S., Lombardi, M., Atzeni, E., et al. (2017). Overview on additive manufacturing technologies. *Proceedings of the IEEE, 105*, 593–612.
Chen, J., Mu, T., Goffin, D., Blecker, C., Richard, G., Richel, A., et al. (2019). Application of soy protein isolate and hydrocolloids based mixtures as promising food material in 3D food printing. *Journal of Food Engineering, 261*, 76–86.
Chen, Y., Zhang, M., & Phuhongsung, P. (2021). 3D printing of protein-based composite fruit and vegetable gel system. *LWT, 141*, 110978.
Chokshi, D. (2006). Toxicity studies of Blockal, a dietary supplement containing phase 2 starch neutralizer (Phase 2), a standardized extract of the common white kidney bean (*Phaseolus vulgaris*). *International Journal of Toxicology, 25*, 361–371.
Dai, B., & Matsukawa, S. (2012). NMR studies of the gelation mechanism and molecular dynamics in agar solutions. *Food Hydrocolloids, 26*, 181–186.
Fan, H., Zhang, M., Liu, Z., & Ye, Y. (2020). Effect of microwave-salt synergetic pre-treatment on the 3D printing performance of SPI-strawberry ink system. *LWT- Food Science and Technology, 122*, 109004.
Gao, L., Dai, W., Chen, J., Xie, Z., & Yue, X. (2017). Enhanced electro-responsive behaviors of agar/xanthan gum interpenetrating compound hydrogel. *Soft Materials, 15*, 163–172.
Guo, W. H., Guan, E. Q., Ke, B., & Zhan, J. L. (2015). Effects of superfine grinding technology on the functional properties of peanut protein. *Journal of Henan University of Technology (Natural Science Edition), 36*, 52–56 (In chinese).
Holland, S., Tuck, C., & Foster, T. (2018). Selective recrystallization of cellulose composite powders and microstructure creation through 3D binder jetting. *Carbohydrate Polymers, 200*, 229–238.
Huang, X., Liang, K. H., Liu, Q., Qiu, J., & Zhu, H. (2020). Superfine grinding affects physicochemical, thermal and structural properties of Moringa Oleifera leaf powders. *Industrial Crops and Products, 151*, 112472.
Hu, J., Chen, Y., & Ni, D. (2012). Effect of superfine grinding on quality and antioxidant property of fine green tea powders. *Lebensmittel-Wissenschaft und -Technologie- Food Science and Technology, 45*, 8–12.
Hussain, S., Malakar, S., & Arora, V. K. (2021). Extrusion-based 3D food printing: Technological approaches, material characteristics, printing stability, and post-processing. *Food Engineering Reviews*. https://doi.org/10.1007/s12393-021-09293-w
Jiang, H., Zheng, L., Zou, Y., Tong, Z., Han, S., & Wang, S. (2019). 3D food printing: Main components selection by considering rheological properties. *Critical Reviews in Food Science and Nutrition, 59*, 2335–2347.
Lee, C. P., Karyappa, R., & Hashimoto, M. (2020). 3D printing of milk-based product. *RSC Advances, 10*, 29821–29828.
Lee, J. H., Won, D. J., Kim, H. W., & Park, H. J. (2019). Effect of particle size on 3D printing performance of the food-ink system with cellular food materials. *Journal of Food Engineering, 256*, 1–8.

Liu, Z., Bhesh, B., Sangeeta, P., Sylvester, M., & Min, Z. (2018a). Linking rheology and printability of a multicomponent gel system of carrageenan-xanthan-starch in extrusion based additive manufacturing. *Food Hydrocolloids, 87*, 413–424.

Liu, Y. W., Liu, D., Wei, G., Ma, Y., Bhandari, B., & Zhou, P. (2018b). 3D printed milk protein food simulant: Improving the printing performance of milk protein concentration by incorporating whey protein isolate. *Innovative Food Science & Emerging Technologies, 49*, 116–126.

Liu, Y. W., Yi, S., Ye, T., Leng, Y., Alomgir Hossen, M., Sameen, D. E., et al. (2021). Effects of ultrasonic treatment and homogenization on physicochemical properties of okara dietary fibers for 3D printing cookies. *Ultrasonics Sonochemistry, 77*, 105693.

Liu, Z. B., Zhang, M., Bhandari, B., & Yang, C. (2018c). Impact of rheological properties of mashed potatoes on 3D printing. *Journal of Food Engineering, 220*, 76–82.

Maniglia, B. C., Lima, D. C., Junior, M., Oge, A., & Le-Bail, A. (2020). Dry heating treatment: A potential tool to improve the wheat starch properties for 3D food printing application. *Food Research International, 137*, 109731.

Nagar, M., Sharanagat, V. S., Kumar, Y., Singh, L., & Mani, S. (2019). Influence of xanthan and agar-agar on thermo-functional, morphological, pasting and rheological properties of elephant foot yam (*Amorphophallus paeoniifolius*) starch. *International Journal of Biological Macromolecules, 136*, 831–838.

Nayar, V. T., Weiland, J. D., Nelson, C. S., & Hodge, A. M. (2012). Elastic and viscoelastic characterization of agar. *Journal of the Mechanical Behavior of Biomedical Materials, 7*, 60–68.

Nida, S., Anukiruthika, T., Moses, J. A., & Anandharamakrishnan, C. (2021). 3D printing of grinding and milling fractions of rice husk. *Waste and Biomass Valorization, 12*, 81–90.

Shi, Z., Zhang, X., Zhu, Y., Yao, Y., & Ren, G. (2021). Natural extracts from white common bean (*Phaseolus Vulgaris* L.) inhibit 3T3-L1 adipocytes differentiation. *Applied Sciences, 11*, 167.

Shi, Z., Zhu, Y., Teng, C., Yao, Y., Ren, G., & Richel, A. (2020). Anti-obesity effects of α-amylase inhibitor enriched-extract from white common beans (*Phaseolus vulgaris* L.) associated with the modulation of gut microbiota composition in high-fat diet-induced obese rats. *Food & Function, 11*, 1624–1634.

Sun, C., Liu, R., Ni, K., Wu, T., Luo, X., Liang, B., et al. (2016). Reduction of particle size based on superfine grinding: Effects on structure, rheological and gelling properties of whey protein concentrate. *Journal of Food Engineering, 186*, 69–76.

Sun, C., Liu, R., Wu, T., Liang, B., Shi, C., & Zhang, M. (2015). Effect of superfine grinding on the structural and physicochemical properties of whey protein and applications for microparticulated proteins. *Food Science and Biotechnology, 24*, 1637–1643.

Tarhan, O., Spotti, M. J., Schaffter, S., Corvalan, C. M., & Campanella, O. H. (2016). Rheological and structural characterization of whey protein gelation induced by enzymatic hydrolysis. *Food Hydrocolloids, 61*, 211–220.

Ulfa, G. M., Putri, W. D. R., Fibrianto, K., Prihatiningtyas, R., & Widjanarko, S. B. (2020). The influence of temperature in swelling power, solubility, and water binding capacity of pregelatinised sweet potato starch. *IOP Conference Series: Earth and Environmental Science, 475*, Article 012036.

Ullah, I., Yin, T., Xiong, S., Huang, Q., Zia-ud-Din, Zhang, J., et al. (2018). Effects of thermal pre-treatment on physicochemical properties of nano-sized okara (soybean residue) insoluble dietary fiber prepared by wet media milling. *Journal of Food Engineering, 237*, 18–26.

Wang, C., Li, T., Ma, L., Li, T., Yu, H., Hou, J., et al. (2020). Consequences of superfine grinding treatment on structure, physicochemical and rheological properties of transglutaminase-crosslinked whey protein isolate. *Food Chemistry, 309*, 125757.

Yang, F., Zhang, M., Bhandari, B., & Liu, Y. (2018). Investigation on lemon juice gel as food material for 3D printing and optimization of printing parameters. *Lwt- Food Science and Technology, 87*, 67–76.

Yang, M. Y., Zhang, X. Q., Ma, Y., Shen, J., Song, J. R., & Zhu, H. L. (2008). Purification and partial characterization of a glycoprotein alpha-amylase inhibitor from white kidney bean (*phaseolus vulgaris*. L). *Journal of Food Biochemistry, 32*, 72–84.

Yao, Y., Hu, Y., Zhu, Y., Gao, Y., & Ren, G. (2016). Comparisons of phaseolin type and α-amylase inhibitor in common bean (*Phaseolus vulgaris*. L.) in China. *Crop Journal, 4*, 68–72.

Zhang, L., Lou, Y., & Schutyser, M. (2018). 3D printing of cereal-based food structures containing probiotics. *Food Structure, 18*, 14.

Zhu, Y., Dong, L., Huang, L., Shi, Z., Dong, J., Yao, Y., et al. (2020). Effects of oat β-glucan, oat resistant starch, and the whole oat flour on insulin resistance, inflammation, and gut microbiota in high-fat-diet-induced type 2 diabetic rats. *Journal of Functional Foods, 690*, 103939.

Zhu, S., Stieger, M. A., van der Goot, A. J., & Schutyser, M. A. I. (2019). Extrusion-based 3D printing of food pastes: Correlating rheological properties with printing behaviour. *Innovative Food Science & Emerging Technologies, 58*, 102214.

Zi, Y., Wang, C., Chen, X., Chen, T., Li, X., Hao, Z., et al. (2015). Preparation and thermal stability of white kidney bean polypeptide with α-amylase inhibitory activity, 2015 *Food Science, 13*, 190–195 (In chinese).